Vector analyzing power iT_{11} in the $\pi^+ d \rightarrow pp$ reaction in the energy region $T_\pi = 350$–450 MeV

N. A. Bazhanov, V. A. Efimovykh, O. Ya. Fedorov, S. I. Kalentarova, A. I. Kovalev, V. I. Murzin, V. E. Popov, A. N. Prokofiev, V. V. Polyakov, A. V. Shvedchikov, V. A. Shchedrov, V. Yu. Trautman, V. G. Vovchenko, and A. A. Zhdanov
St. Petersburg Nuclear Physics Institute, Gatchina, Russia

E. I. Bunyatova, Yu. M. Kazarinov, and Yu. A. Usov
Joint Institute of Nuclear Research, Dubna, Russia

E. Boschitz, B. Brinkmöller, and M. Wessler
University of Karlsruhe, Karlsruhe, Federal Republic of Germany
(Received 2 December 1991)

The vector analyzing power iT_{11} of the reaction $\pi d \rightarrow pp$ was measured at $T_\pi = 350$, 400, and 450 MeV. The results obtained at $T_\pi = 350$ MeV are in agreement with earlier measurements of iT_{11} at 325 MeV. With increasing energies our results show a marked increase in the vector analyzing power up to a value close to its theoretical limit at $T_\pi = 450$ MeV ($\sqrt{s} = 2.40$ GeV). In this energy region broad structure has been found in earlier measurements of $d\sigma/d\Omega$ and A_{y0}.

PACS number(s): 25.10.+s, 24.70.+s, 25.80.Ls

The reaction $\pi^+ d \rightarrow pp$ and its inverse reaction $pp \rightarrow d\pi^+$ are the main processes of pion absorption and production at intermediate energies. Accordingly a lot of effort, both theoretically and experimentally, was made to investigate this reaction. On the theoretical side several groups tried to understand the process in the larger framework of the πNN system, with the aim to explain all of the various reactions $NN \rightarrow NN$, $NN \leftrightarrow \pi d$, $NN \rightarrow \pi NN$, $\pi d \rightarrow \pi NN$, and $\pi d \rightarrow \pi d$ simultaneously [1]. Although some of the main features of the various channels are well reproduced by such calculations, there exist serious discrepancies between predictions and measurements of many of the more sensitive polarization parameters.

It is at the moment not clear how to overcome the obvious shortcomings of the theoretical calculations [2]. One way to find possible common causes for the discrepancies between experiment and theory is by phase-shift analyses or by direct reconstruction of the helicity amplitudes [3] for the different channels. For the $\pi^+ d \leftrightarrow pp$ reaction six independent helicity amplitudes are needed, so eleven measurements at a given energy and scattering angle (differential cross section and ten spin observables) are required to fully determine these amplitudes within a common phase. Below $T_p = 800$ MeV ($\sqrt{s} = 2.24$ GeV) nearly complete data sets exist for those spin observables that can be measured with a polarized proton beam and target [4]. Together with the measurement of iT_{11} for the reaction $\pi d \rightarrow pp$ [5] at least the larger amplitudes below this energy could be fixed within reasonable error bands [6]. The recently reported measurements of spin transfer observables of the $\pi \vec{d} \rightarrow \vec{p}p$ reaction will reduce the remaining uncertainties considerably [7].

At higher energies only few measurements exist. Total and differential cross sections have been measured up to an energy $T_\pi = 1$ GeV ($\sqrt{s} = 2.80$ GeV) and the results obtained for different energies and at different laboratories can be parametrized in a consistent way [8]. Several angular distributions of A_{y0} up to $T_p = 2.3$ GeV ($\sqrt{s} = 2.8$ GeV) have also been measured [9–12].

The A_{y0} as well as the differential cross section data show evidence of broad structure at $\sqrt{s} = 2.41$ GeV [13] and 2.66 GeV [11, 12]. The origin of this structure is not known at present. It might be due to an accidental conspiracy of several nondominant partial waves, but threshold effects or more exotic effects such as dibaryons are also discussed [13].

To prove or disprove these possibilities, more data on other spin observables in the same energy region are necessary. We therefore decided to measure the vector analyzing power iT_{11} at $T_\pi = 350$, 400, and 450 MeV ($\sqrt{s} = 2.32$, 2.36, and 2.40 GeV) using a polarized deuterium target at the pion channel of the St. Petersburg Nuclear Physics Institute. These measurements extend the energy range of data taken at the Paul Scherrer Institut (PSI) [5] to higher energies, and together with them give a good description of the energy dependence of this observable up to the energy of the first observed irregularity.

The vector analyzing power (iT_{11}) can be measured either as the polarization of a final deuteron in the $pp \rightarrow d\pi^+$ reaction or as an asymmetry with a pion beam and a polarized deuteron target in the $\pi^+ d \rightarrow pp$ reaction. We used the second approach, which utilizes a polarized deuteron target in a single scattering experiment with a pion beam. The cross section of this reaction can be expressed as

$$\sigma^{\pm} = \sigma^0 \left[1 \pm \sqrt{3} i T_{11} \mathrm{P}_z^{\pm} - \frac{\sqrt{3}}{2} P_{zz} \left(T_{22} + \frac{T_{20}}{\sqrt{6}} \right) \right] \quad (1)$$

where σ^+, σ^-, σ^0 are the cross sections for different target polarizations (+,−,zero), P_z and P_{zz} are the vector and tensor target polarizations, and iT_{11}, T_{22}, T_{20} are vector analyzing power and different components of the tensor analyzing power. In the case $P_z^+ = P_z^-$ we obtain for the vector analyzing power

$$iT_{11} = \frac{1}{2\sqrt{3}} \frac{1}{P_z} \frac{\sigma^+ - \sigma^-}{\sigma^0}. \quad (2)$$

The polarized deuterium target we used was made from 1.5-mm-diameter beads of fully deuterated propandiol $C_3O_2D_8$, chemically doped with a Cr(V) complex. The polarization was achieved by dynamic nuclear polarization in a dilution refrigerator inside a 2.5 T magnetic field. The magnetic field was provided by a split-coil superconducting solenoid with 406 mm diameter and a 30 mm gap between the coils. In the center of the solenoid there was a stainless-steel cylindrical vessel filled with ^{4}He at 4.2 K. Inserted in this vessel was the appendix of a dilution refrigerator with a mixing chamber. This mixing chamber contained a gold-plated brass resonator which itself contained the target beads. The target material was kept in place from the top and the bottom by perforated teflon covers. The target was of cylindrical shape with the axis aligned perpendicular to the scattering plane. The target diameter was 27.3 mm and the height 27 mm. The target cell contained 10.2 ± 0.2 g of propandiol, which gives an average target thickness of 1.3 g/cm^2. This has to be compared with the total thickness of all materials surrounding the target of about 0.6 g/cm^2.

During the data runs the target was kept in frozen spin mode with the magnetic field at 2.5 T. The polarization was measured before and after each run by recording the NMR absorption spectrum of the deuteron. This was done, using a Q meter with a series circuit and a phase shift detector to provide small corrections due the influence of dispersion and nonlinearities [14]. The NMR spectrum consists of two overlapping lines. The intensity of each line was measured using the method described in Ref. [15]. The polarization can be determined from the ratio of these intensities. The average polarizations obtained for the deuterons were between 0.37 and 0.40. The relative precision of the measurements is between 2.5% and 5%.

For the runs with zero polarization the mixing chamber temperature was increased to about 0.4 K and the magnetic field was reduced to zero. Then the temperature and magnetic field values of the runs with polarization were restored and the polarization was checked. No NMR signal was found above noise level, which corresponds to a polarization less than 0.01.

One of the difficulties in this measurement is the presence of background materials inside the target (^{12}C, ^{16}O) or placed around it (^{3,4}He, Cu, Fe, ...). The background has to be subtracted by explicit measurements with a dummy target and without any target, to determine the background coming from the magnetic and cryogenic systems surrounding the target.

Two dummy targets were used for the background measurements in this experiment. The first one consisted of four plates of carbon with the density $\rho = 1.93$ g/cm^3. The amount of carbon and of helium in this dummy target was chosen to obtain a mass ratio

$$\frac{M'_{\mathrm{He}}}{M'_{\mathrm{C}}} = \frac{M_{\mathrm{He}}}{M_{\mathrm{C}} + M_{\mathrm{O}}}, \quad (3)$$

where M'_i and M_i (i = He, C, O) are the masses of the corresponding elements in the dummy target and in the polarized target, respectively.

The second dummy target consisted of a mixture of beads of frozen CO_2 and carbon to obtain equal amounts of carbon and oxygen in the dummy target and in the polarized target. However, as the density of the dummy target material is two times larger than that of propandiol, the mass of liquid helium was larger in the dummy target than in the polarized one. This was taken into account by an additional measurement using the dummy target without helium.

The pion channel of the St. Petersburg Nuclear Physics Institute synchrocyclotron and the layout of the installation used in our experiment are presented in Fig. 1. The 1-GeV proton beam extracted from the synchrocyclotron was directed at a berylium pion production target of 17 cm length and 5 cm diameter. Pions produced at 0° were focused using a system of quadrupoles Q_1–Q_7, analyzed by the dipole magnets M_1 and M_2 and directed at the polarized target. The dispersion of the beam depends on the width of the slit in the C_1 collimator which is placed at the intermediate focus of the magnetic system and was chosen to obtain maximum intensity of the beam, which restricts the momentum resolution of the channel to 5.8%.

The intensity of the pion beam varied with the pion momentum and was between 2.5×10^5 and 3.5×10^5 pions per second. The beam was shaped to obtain maximum intensity on an area corresponding to the size of the polarized target. This was done in a separate run with a scintillation detector installed in the position of the target. Under these conditions, the pion flux on the polarized target was between 1.0×10^5 and 1.5×10^5 pions per second. The position of the beam on the polarized target was checked by proton beam radiography. The scintillation detectors S_1–S_4 were used as beam monitors. The scintillator S_4 had a hole in the middle that matched the size of the polarized target and was used to suppress background due to the beam halo.

The pion beam has an admixture of μ^+ mesons of less than 4.2% and of e^+ less than 1.5%. The proton content of the beam transported to the polarized target was about 10–15 % of the total intensity. Time of flight information over the distance of 1.5 m between the scintillators S_1 and S_2 reduces this to a level of 1.5–3 %. The investigated process ($\pi^+ d \to pp$) was separated from the events coming from pd-elastic and pp-quasielastic scattering by using kinematical constraints and the measured time of flight and the energy loss of the outgoing particles.

The system for secondary particles registration consisted of scintillation detectors S_5–S_8 mounted near the polarized target cryostat and hodoscopes H_1–H_4 mounted 1 meter behind the scintillators. Each ho-

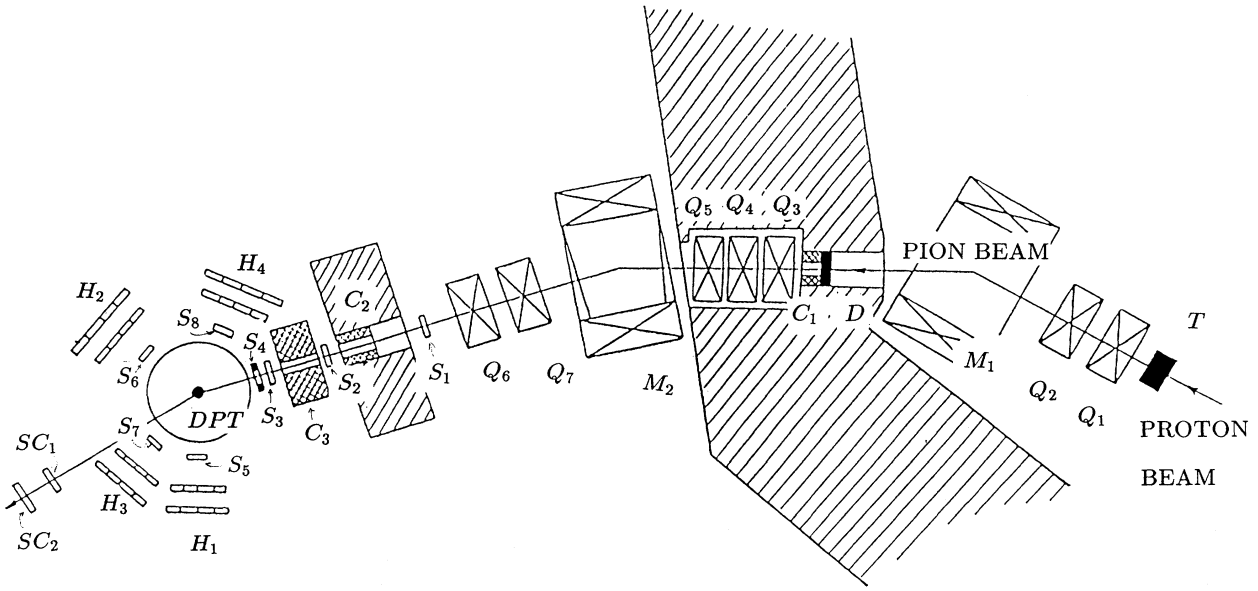

FIG. 1. Experimental layout. T, pion production target; Q_1–Q_7, quadrupoles; M_1 and M_2, dipole magnets; D, degrader; C_1–C_3, collimators; S_1–S_8 and SC_1 and SC_2, scintillation detectors; H_1–H_4, hodoscopes; DPT, deuteron polarized target.

doscope consisted of four pairs of scintillation detectors. The first row of detectors was used for time-of-flight measurements. The second row consisted of 1-cm-thick plastic scintillators and provided the information on the energy loss of the particles. The angular acceptance in the reaction plane was $\Delta\Theta_{\rm lab} \simeq 4°$ for each detector pair. The azimuthal acceptance $\Delta\phi \simeq 7.5°$ to $8.6°$ was chosen to agree with the size of the gap between the coils of polarized target solenoid.

The four hodoscopes could be rotated together with the corresponding scintillation detectors around the target position. Before the start of the experiment all hodoscopes were calibrated in the direct pion beam which was enriched by protons. This calibration was repeated in the middle and at the end of the experiment. The beam momentum used for the calibration measurements was 573 MeV/c (T_π = 450 MeV, T_p = 160 MeV). For the measurement of the asymmetry the hodoscopes were placed at two kinematically conjugate angle pairs determined by the kinematics of the $\pi^+ d \rightarrow pp$ reaction. The deflection of the pion beam and the outgoing protons was taken into account for the placement of the detectors. For T_π = 450 MeV these deflections were 6.4° for the pions and 3.5°–7.0° for the outgoing protons. The event trigger was defined by a coincidence from the beam counters S_1, S_2, and S_3 with signals from the conjugate detector arms S_5 and S_6 or S_7 and S_8. Also required was the absence of a signal from the counter S_4.

At 450 MeV measurements with both dummy targets were carried out. The results agreed within the statistical uncertainty. For the measurements at 350 and 400 MeV only the second dummy target was used. Figure 2 shows an example of the measured spectra using the polarized target and a dummy target. Besides contributions from the $\pi d \rightarrow pp$ reaction (centered at channel 24 in the spectra of Fig. 2) there are large contributions from (π, p) quasifree scattering (centered at channel 7). At each energy and angle we measured the yield for positive, negative, and zero target polarization (N^+, N^-, and N^0), as well as the yield from the dummy target (N^d) and the run without target (N^e). The measurements were carried out in the sequence N^+, N^-, N^-, N^+, N^0, N^d, N^e. The stability of the measurements was checked using the count rate ratios of various beam monitors, as well as the ratios of the monitor numbers to the number of recorded events for all pairs of detectors in the hodoscopes. All these ratios were stable within the statistical accuracy.

Figure 3 shows the angular distributions obtained at

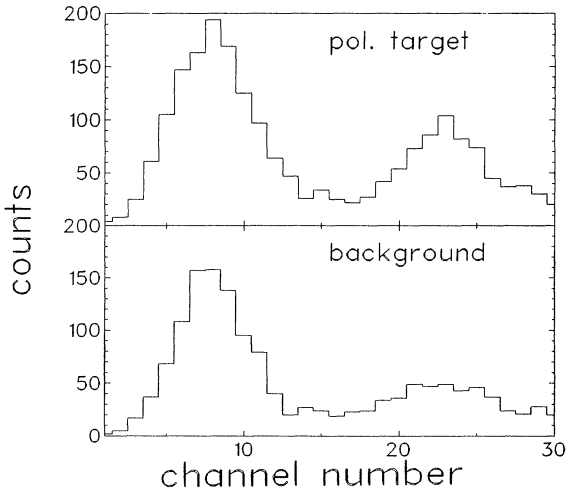

FIG. 2. Spectra measured with a hodoscope for the polarized target and a dummy target at T_π = 350 MeV and $\Theta_{\rm c.m.}$ = 40°. Shown is a projection of the two-dimensional dE/dx, TOF spectrum that gives the best separation of the two dominating processes. The peak centered at channel 7 is due to quasifree πp scattering, the peak centered at channel 24 is dominated by contributions from the $\pi d \rightarrow pp$ reaction.

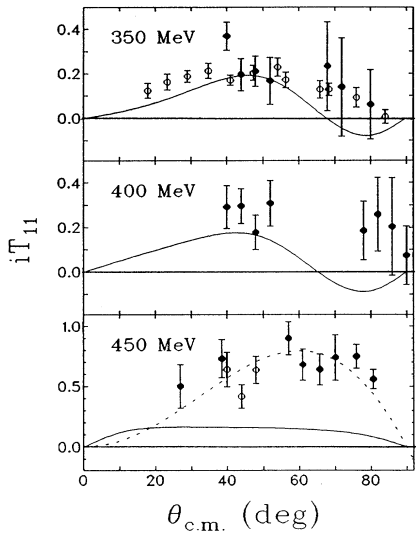

FIG. 3. Angular distribution of the vector analyzing power iT_{11} for the $\pi^+ d \rightarrow pp$ reaction at T_π = 350, 400, and 450 MeV. Our results for T_π = 350 MeV (full circles) are shown together with the results from Ref. [5] at T_π = 325 MeV (open circles). For T_π = 450 MeV open and full circles denote results from two different runs. The solid curve is a prediction from the partial-wave analysis of Ref. [15]. The dashed curve is to guide the eye.

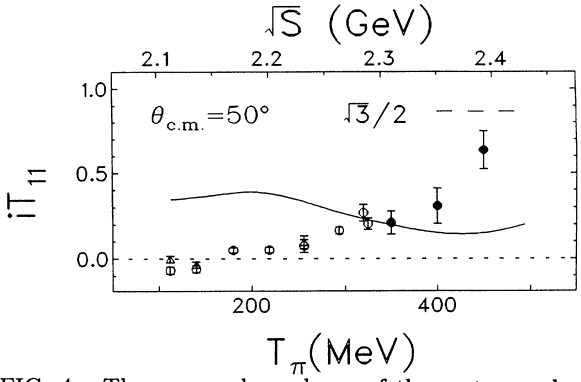

FIG. 4. The energy dependence of the vector analyzing power iT_{11} for the $\pi^+ d \rightarrow pp$ reaction at $\Theta_{c.m.}$ = 50°. Open circles denote results from measurements at PSI [5], full circles are results from this measurement. The solid curve is a prediction from the partial-wave analysis of Ref. [15]. The long dashed curve indicates the theoretical limit for iT_{11}.

350, 400, and 450 MeV. Our results at T_π = 350 MeV are plotted together with the results obtained at T_π = 325 MeV from an earlier PSI measurement [5]. The phase shift analysis predicts only minor changes in this energy region and the measurements at PSI show only a very weak energy dependence below T_π = 325 MeV. Therefore it is expected that the two measurements coincide, which is the case. The extrapolation of the measured value for iT_{11} to $\Theta_{c.m.}$ = 90° is also consistent with zero, as is required by the symmetry of the final state of the reaction.

The data obtained at T_π = 450 MeV ($\sqrt{s}$ = 2.4 GeV) show a rise of iT_{11} up to a level close to its theoretical limit ($\sqrt{3}/2$). Because of the unexpectedly large value for iT_{11} found in a first measurement at T_π = 450 MeV, a second measurement was done. Both measurements were consistent with each other.

Also shown in Fig. 3 are predictions from a first energy-dependent phase shift analysis [16]. The agreement with the data is rather good at T_π = 350 MeV and still not too bad at 400 MeV, whereas at 450 MeV the prediction is in complete disagreement with the data. One has to point out, however, that this analysis was done before the iT_{11} measurements at lower energies [5] became available. It is in serious disagreement with the data on iT_{11} at lower energies also, so that the rather good agreement at T_π = 350 MeV is somewhat accidental. Other analyses, that give a better description at lower energies [6], do not cover the energy range of our experiment. Also theoretical calculations are not yet available.

The dramatic rise of the vector analyzing power as a function of pion energy is made evident in the excitation function shown in Fig. 4 for iT_{11} near the maximum of the angular distribution at $\Theta_{c.m.}$ = 50°. Comparing this energy dependence with the energy dependence of the differential cross section [13] and of A_{y0} [11, 12], one finds all sets of data show evidence of structure near $\sqrt{s}$ = 2.41 GeV. The experimental data gathered so far for this reaction in this energy region is not enough to perform a detailed phase-shift analysis. However, it seems worthwhile to try another energy-dependent analysis as in Ref. [16] that uses analyticity and measurements at lower energies to restrict the amplitudes.

[1] M. Garcilazo and T. Mizutani, *πNN Systems* (World Scientific, New York, 1990), and references therein.
[2] B. Blankleider, PSI Report No. PSI-PR-91-01, 1991 (unpublished).
[3] M. P. Locher, M. E. Saino, and A. Švarc, Adv. Nucl. Phys. **17**, 47 (1986).
[4] D. V. Bugg, J. Phys. G. **10**, 717 (1984).
[5] G. R. Smith *et al.*, Phys. Rev. C **30**, 980 (1984).
[6] D. V. Bugg, Nucl. Phys. A **437**, 534 (1985).
[7] A. Feltham *et al.*, Phys. Rev. Lett. **22**, 2573 (1991).
[8] B. G. Ritchie, Phys. Rev. C **44**, 553 (1991).
[9] M. D. Corcoran *et al.*, Phys. Lett. **120B**, 309 (1983).
[10] B. Mayer *et al.*, Nucl. Phys. A **437**, 630 (1985).
[11] R. Bertini *et al.*, Phys. Lett. **162B**, 77 (1985).
[12] R. Bertini *et al.*, Phys. Lett. B **203**, 18 (1988).
[13] B. L. G. Bakker and I. I. Strakovsky, Nucl. Phys. A **505**, 551 (1989).
[14] N. A. Bazhanov and A. I. Kovaljov, in *Proceedings of the 9th International Symposium of High Energy Spin Physics, Bonn, Federal Republic of Germany, 1990*, edited by W. Meyer, E. Steffens, and W. Thiel (Springer, Berlin, 1991), Vol. 2, p. 261.
[15] Yu. F. Kiselev, V. V. Polyakov, A. I. Kovalev, E. I. Bunyatova, N. S. Borisov, V. Yu. Trautman, K. Werner, and N. G. Kozlenko, Nucl. Instrum. Methods. Phys. Res. **220**, 399 (1984).
[16] A. V. Kravtsov, M. G. Ryskin, and I. I. Strakovsky, J. Phys. G. **9**, L187 (1983); LNPI Report No. 963, 1984 (unpublished).